An improved N-body semi-empirical model for body-centred cubic transition metals

G. J. Ackland & R. Thetford

An improved *N*-body semi-empirical model for body-centred cubic transition metals

By G. J. ACKLAND† and R. THETFORD

Theoretical Physics Division, Harwell Laboratory,
Oxfordshire OX11 0RA, England

ABSTRACT

The recently published semi-empirical potentials of Finnis and Sinclair for the metals V, Nb, Ta, Mo and W appear to give unphysical results for properties involving small interatomic separation. This is remedied by adding to the potentials cores fitted to electron gas calculations on dimers. The adjusted potentials are shown to predict a more realistic pressure–volume relationship. Interstitial formation energies are calculated for various configurations, using quenched molecular dynamics and static relaxation. Some preliminary results on interstitial migration are presented.

§ 1. INTRODUCTION

In the atomistic modelling of transition metals, pair potentials have been found to be insufficient to explain a number of observations. In any purely pairwise model, the Cauchy pressure $\frac{1}{2}(C_{12} - C_{44})$ (where C_{12} and C_{44} are components of the elastic modulus tensor) is necessarily zero, and the free surface of a metal shows an outward relaxation, contrary to experiment. With such drawbacks it became clear that a different approach was required.

The *N*-body potentials developed by Finnis and Sinclair (FS) (1984) have been used successfully to calculate properties of vacancies (Matthai and Bacon 1985, Maysenhölder 1986) and surfaces (Ackland and Finnis 1986) in several b.c.c. transition metals. However, the parameters fitted from the equilibrium state led to anomalies in properties for which atoms are forced close together, such as the compressibility at high pressure. Two of the potentials, for vanadium and niobium, are actually attractive at short range. This causes problems in molecular dynamics (MD) calculations as the atoms tend to fall together.

In this paper we describe an alteration of the form of the FS potentials for V, Nb, Ta, Mo and W, at short range. This overcomes the anomalies mentioned above, without changing the fitting to elastic constants at the near-equilibrium positions. It has been achieved by adding a core term to the pairwise repulsive part of the FS potential to increase the short-range repulsion. This term has roughly exponential form and is fitted to the electron gas potentials for dimers described in § 3.

Once the new potentials have been derived, we apply them in a number of cases to calculate pressure–volume relationships, dimer energies and interstitial energies and relaxations. These results are compared, where possible, with calculations using the FS potentials without the cores.

---

† University of Oxford, Department of Theoretical Physics, 1 Keble Road, Oxford OX1 3NP, England.

§ 2. THE MODEL

The model of the energy due to Finnis and Sinclair (1984) comprises an attractive many-body term and a repulsive pair potential. The total energy of the configuration of atoms is written as

$$U_{\text{tot}} = U_N + \frac{1}{2} \sum_{ij} V_{\text{FS}}(R_{ij}). \tag{1}$$

The second term is a conventional pair-potential summation, and the N–body term has the form

$$U_N = -A \sum_i \left(\sum_j \phi(R_{ij}) \right)^{1/2}. \tag{2}$$

The above energy functions were parameterized in a purely empirical way by FS, thus

$$\phi(r) \begin{cases} = (r-d)^2 & r \leqslant d \\ = 0 & r > d. \end{cases} \tag{3}$$

$$V_{\text{FS}}(r) \begin{cases} = (r-c)^2(c_0 + c_1 r + c_2 r^2) & r \leqslant c \\ = 0 & r > c. \end{cases} \tag{4}$$

The cutoffs d and c were chosen to lie between the second and third neighbour separations in the b.c.c. structure for which parameters were fitted.

§ 3. FITTING THE CORE TO ELECTRON-GAS POTENTIALS

The electron-gas method of calculating interatomic forces was originally proposed by Jensen (1932, 1936) and Lenz (1932) and has been used frequently since then, notably by Wedepohl (1967), and by Gordon and Kim (1972) by whose names the method is now most frequently known. The total energy of interacting atoms is written as a sum of Coulombic, kinetic, exchange and correlation energies, The latter three terms are assumed to be functions of the local charge density. The electronic structures of the isolated atoms are calculated accurately using a Hartree–Fock scheme (Herman and Skillman 1963). When the atoms are brought together, the total energy is calculated from a charge density which is a simple superposition of the individual atomic densities.

The programs used to evaluate the electron gas potentials are those described by Harding and Harker (1982), and for a detailed description the reader is referred to their work. The calculation produces potentials describing a dimer of singly charged ions. This approach is used because the 4s electron is assumed to be delocalized. Naturally when calculating the Coulombic energy using ionic charge densities it is necessary to subtract the excess core–core repulsion.

The form of the electron-gas potential is roughly exponential. We aim to fit an analytic function to the numerical values of energy versus dimer separation produced by the program. The force on each atom is calculated by numerical differentiation and interpolation.

The short-range part of the FS potential was adjusted to fit this interatomic potential, with the Coulombic part due to the excess nuclear charge subtracted. In the fitting a number of criteria were adhered to:

(1) As the original FS model is fitted to elastic constants at equilibrium atomic separations, the core was designed to be short-range with a cutoff inside the

metallic nearest-neighbour distance. This ensures that the elastic constants are unaffected.

(2) The core was fitted to the forces, rather than the energies, deduced from the electron-gas potential. This avoids problems with a mismatch between the energies at the cutoff of the core.

(3) In order to ensure a smooth pressure–volume relation, it was necessary that the added core function and its derivatives go to zero at the cutoff.

(4) The potential is intended for simulation of defects, for example with molecular dynamics calculations. Thus it is designed to be most accurate in the lower energy range, near to equilibrium separations, where the atoms are more likely to be found.

To satisfy this last criterion a least-relative-squares fit was used. Several different functional forms were tried, and the one which best fitted the data while satisfying all the criteria was a product of a cubic and an exponential term:

$$V(R_{ij}) = V_{FS}(R_{ij}) + B(b_0 - R_{ij})^3 \exp(-\alpha R_{ij}). \tag{5}$$

The parameters B and α as determined from fitting in the region $0.4 < R_{ij}/b_0 < 1.0$ are shown in table 1, together with the nearest-neighbour distances b_0. The accuracy of the fitting varied considerably. In molybdenum, fig. 1 shows that the extrapolation of the FS polynomials was very similar to the electron-gas potential. As $R_{ij} \to b_0$, the difference between the two goes to zero faster for Mo than for the other metals (figs. 2–4), which leads to a larger value of α. With a large negative exponential, the pre-exponential factor B can be large without implying a drastic correction to the FS potentials. The relative-squares fit was accurate to within about 0.2% throughout the fitted region. In vanadium there was a much greater difference between the FS extrapolation and the electron gas potential, and the fit was accurate only to within about 4%.

Table 1. Parameters of the core function in eqn. (5).

| Metal	B (eV Å^{-3})	α (Å^{-1})	b_0 (Å)
V	23.0	0.5	2.6320
Nb	48.0	0.8	2.8585
Ta	91.0	1.05	2.8629
Mo	1223.0	3.9	2.7255
W	90.3	1.2	2.7411

§4. PRESSURE–VOLUME RELATIONSHIPS

The pressure–volume relationship for FS metals under compression was evaluated analytically, by evaluating the differential of the energy with respect to the lattice parameter. The results are plotted as the broken lines in figs. 1–4. The curve for niobium is very similar to that for vanadium, and has been omitted. There is a large scatter in the experimental data for the form of the pressure–volume curve at extremely high pressures (Bolef 1961, Graham, Nadler and Chang 1968, Carter, Marsh, Fritz and McQueen 1971, Leisure, Hsu and Seiber 1973, Katahara, Manghanani and Fisher 1976, Bell, Shaner and Steinberg 1978, Merx and Moussin 1980, Xu, Mao and Bell 1984), but all results show a monotonic increase in pressure with decreasing volume.

Fig. 1
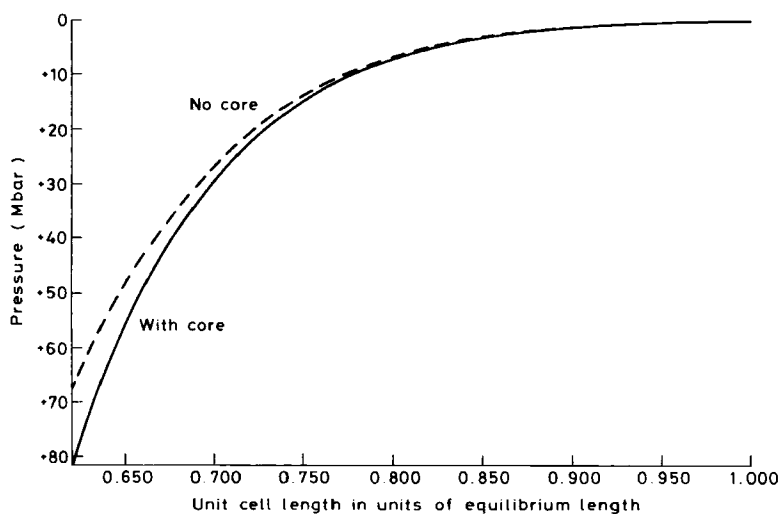
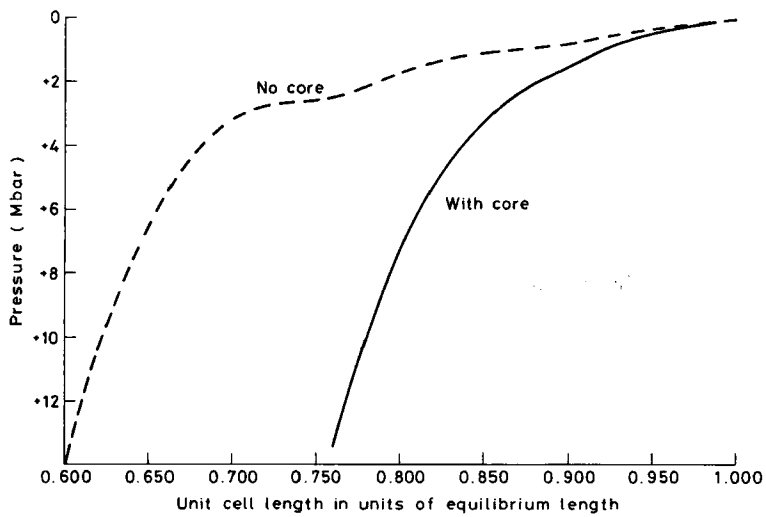Pressure–volume curves for molybdenum.

Fig. 2
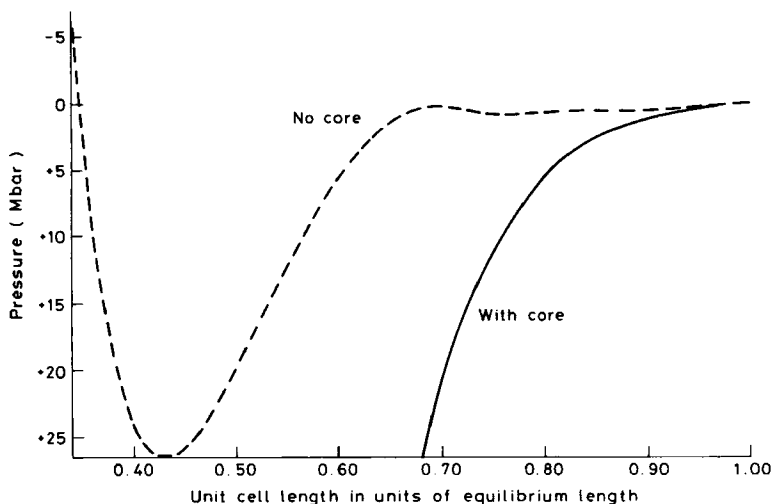
Pressure–volume curves for vanadium.

The results obtained from the unmodified FS potentials are clearly unphysical. Only Mo and W vary monotonically, and at low separations (for nearest-neighbour distances below 0·4 times the equilibrium), V and Nb actually have negative pressure which would cause atoms coming close enough to collapse together. These departures from the expected form are obviously spurious and it is necessary to introduce a core potential to remedy the problem.

Fig. 3

Pressure–volume curves for tantalum.

Fig. 4
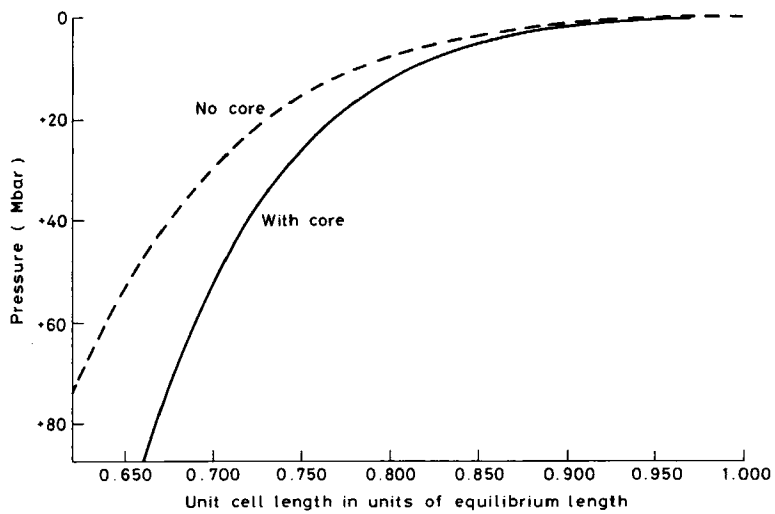
Pressure–volume curves for tungsten.

The pressure–volume curves obtained using the cores are shown as solid lines in figs. 1–4. These are in much better agreement with the expected forms, showing none of the anomalies of the broken curves.

§5. DIMER ENERGIES

A good prediction of dimer energies is encouraging for applications where the coordination is low, for example, the modelling of surface adatoms or of sputtering. Since the potential is fitted to bulk properties, there are two possible approaches to calculating the dimer energy. Firstly, the potential can be applied to a system consisting of only two atoms. The energy then is of the simple form

$$U_{\text{DIMER}}(R_{12}) = V(R_{12}) - 2A\sqrt{\phi(R_{12})}. \tag{6}$$

It is debatable whether the FS method, developed for the bulk material, is applicable to an isolated pair of atoms. It is possible to construct an effective pair potential from the FS potential (Finnis and Sinclair 1984). This has the form

$$V_{\text{eff}}(r) = V(r) - A\rho_0^{-1/2}\phi(r), \tag{7}$$

where

$$\rho_0 = \sum_j \phi(R_{ij}^p) \tag{8}$$

is the term in eqn. (2) for an atom i in the bulk of a perfect crystal. This second approach gives a dimer energy of

$$U_{\text{DIMER}}(R_{12}) = V(R_{12}) - A\rho_0^{-1/2}\phi(R_{12}). \tag{9}$$

There is very little difference in the energies derived from these two methods; so eqn. (6), coming direct from the FS idea, was used.

The calculated dimer binding energies and equilibrium bond lengths are given in table 2. The experimental data available for dimers are very limited, and do not cover the metals studied here. However, the results in table 2 show a dissociation energy of about one-half of the metallic cohesive energy, and an interatomic separation of slightly less than the metallic nearest-neighbour distance. These two facts agree with the experimental data of Huber and Herzberg (1979), and the results of the density functional theory calculations of Harris and Jones (1979) for other metals, which are again at variance with the predictions of pair potentials.

Table 2. Dimer binding energies E_{DBE} and equilibrium bond lengths.

Metal	E_{DBE} (eV)	b_{eqm} (Å)
V	1·7753	2·517
Nb	2·6259	2·691
Ta	3·0708	2·754
Mo	2·2174	2·627
W	2·4654	2·734

§6. INTERSTITIAL CALCULATIONS

As interstitials are the defects most likely to be affected by a change in the form of the potential at small separations, modelling them with the new cores was of interest. Using the potentials derived above, relaxation calculations were made for interstitials in V, Nb, Ta, Mo and W. The relaxation was performed using the DEVIL conjugate gradients program, written at Harwell by Norgett and modified by Thetford (1985). No stable structure could be found with the potentials for V and Nb as originally published, but the addition of the core term led to stable interstitial configurations for these metals.

6.1. *Molybdenum and the bent interstitial*

One feature of the old potential which persists is the apparently strange relaxed configuration of the dumb-bell interstitial in molybdenum. Calculation of interstitial formation energies for the various possible symmetry positions (octahedral, tetrahedral, crowdion; $\langle 100 \rangle$, $\langle 110 \rangle$, and $\langle 111 \rangle$ split dumb-bells) of the defect in a b.c.c. lattice suggested that the $\langle 110 \rangle$ split dumb-bell was energetically favoured (Zeper 1986, Harder and Bacon 1986). But by starting the relaxation from a configuration which was asymmetric, and using the potentials in their original form, a relaxed structure with the atoms of the dumb-bell at approximately $a(\pm 0.32 \pm 0.19\,0.00)$ was found (Thetford 1985). This had an energy lower by about $0.05\,eV$ than that of the $\langle 110 \rangle$ interstitial, and its existence was confirmed elsewhere (Zeper 1986, Harder and Bacon 1986).

A block of size $7a \times 7a \times 7a$ consists of 14 lattice planes in each direction, and is referred to as a 14^3 block. A 14^3 block of perfect lattice contains 686 atoms; 16^3 contains 1024 atoms, and 18^3 contains 1458 atoms.

When the core described above was included in the molybdenum potential, two relaxed minima were found. In a 14^3 block with cyclic boundary conditions, one of the minima has the dumb-bell atoms at $a(\pm 0.3166 \pm 0.1978 \pm 0.0235)$ and formation energy $6.983\,eV$; the other dumb-bell is positioned at $a(\pm 0.2653 \pm 0.2630 \pm 0.0559)$ and has energy $6.991\,eV$. Which of the two is obtained depends on the starting configuration. For a 16^3 block, it is possible to relax to $\langle 110 \rangle$, but only by starting very nearby. An energy of $7.033\,eV$ for the dumb-bell at $a(\pm 0.2658 \pm 0.2658 \pm 0.0001)$ is obtained, compared with $6.974\,eV$ for $a(\pm 0.3182 \pm 0.1958 \pm 0.0182)$. The $\langle 110 \rangle$ dumb-bell is at a very shallow minimum in the potential energy. To try to elucidate how this situation arises, we have considered the effect of rotation of the dumb-bell in 3-space. It is sufficient to consider the tetrahedron bounded by the origin and the three principal directions $\langle 100 \rangle$, $\langle 110 \rangle$ and $\langle 111 \rangle$: see fig. 5. The energy can then be plotted against orientation projected on to the 'stereographic triangle' shaded in fig. 5.

For molybdenum, the relaxation at each point was carried out on a 14^3 block with cyclic boundary conditions. The results are in table 3 and compare well with those given by Zeper (1986). Figure 6 is a contour plot of the region round $\langle 110 \rangle$. It can be seen that, although there is a general tendency for the dumb-bell to sit near the $\langle 110 \rangle$ direction, there is a 'moat' running round a slight rise in the energy at that point.

The energy barrier to rotation around the moat is approximately $16\,meV$, compared with the 'knoll' height of about $50\,meV$. At room temperature thermal motion would lead to a mean alignment in the $\langle 110 \rangle$ direction. If this surface represents the true potential energy, it may be difficult to distinguish it experimentally from one with a global minimum at $\langle 110 \rangle$.

Fig. 5
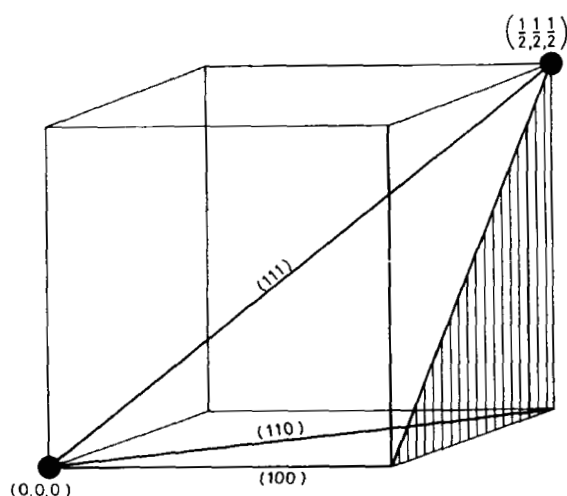
Calculation region for the b.c.c. structure.

Fig. 6
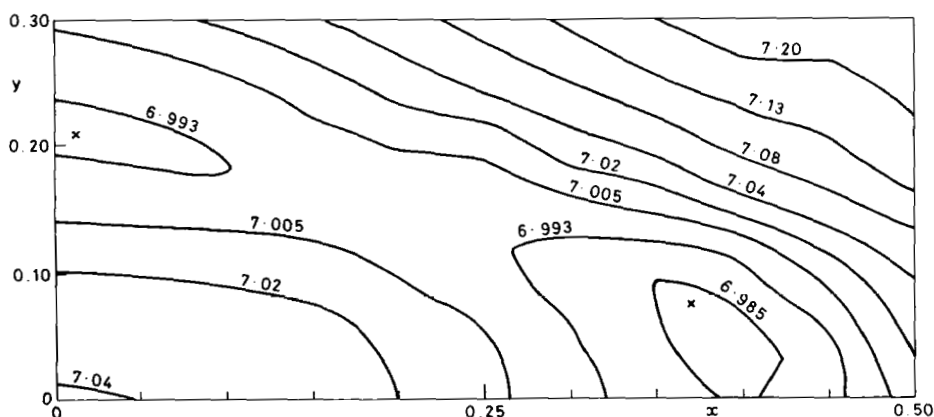
Energy contours (eV) for molybdenum dumb-bell. The dumb-bell orientation is $\langle 1\,1-x\,y\rangle$. Contour levels are chosen to highlight the structure. The two minima are marked with crosses.

6.2. *Tantalum: the effect of the core*

The effect of introducing the core of the potential is most dramatic for tantalum. In fig. 7 we present an energy-orientation diagram for the Ta dumb-bell interstitial before the core was included. To aid interpretation, the energy surface has been reflected in the line joining the points labelled $\langle 100 \rangle$ and $\langle 111 \rangle$: certain features can be clearer in the reflected portion than in the original. The values obtained (see table 3) are broadly in line with those calculated for the principal dumb-bell orientations by Harder and Bacon (1986); we suspect that the slight differences in energy arise from the use of different boundary conditions. The configurations with minimum energy are picked out in bold type.

Table 3. Interstitial formation energies. All blocks have cyclic boundary conditions.

Metal	Configuration	E_i^f (eV)	Core†	Block
V	⟨100⟩	4·963	Y	14^3
V	⟨110⟩	**4·163**	Y	14^3
V	⟨110⟩	**4·155**	Y	16^3
V	⟨111⟩	4·608	Y	14^3
V	Crowdion	4·600	Y	14^3
V	Crowdion	4·592	Y	16^3
Nb	⟨100⟩	4·821	Y	14^3
Nb	⟨110⟩	**4·485**	Y	14^3
Nb	⟨110⟩	**4·472**	Y	16^3
Nb	⟨11	4·795	Y	14^3
Nb	Crowdion	4·857	Y	14^3
Ta	⟨100⟩	8·068	Y	14^3
Ta	⟨110⟩	**6·847**	Y	14^3
Ta	⟨110⟩	**6·828**	Y	16^3
Ta	⟨111⟩	7·157	Y	14^3
Ta	Crowdion	7·158	Y	14^3
Ta	⟨100⟩	4·103	N	14^3
Ta	⟨110⟩	3·968	N	14^3
Ta	⟨111⟩	3·933	N	14^3
Ta	Crowdion	**3·806**	N	14^3
Mo	⟨100⟩	7·207	Y	14^3
Mo	⟨110⟩	7·042	Y	14^3
Mo	⟨110⟩	7·033	Y	16^3
Mo	Bent‡	**6·983**	Y	14^3
Mo	Bent‡	**6·974**	Y	16^3
Mo	⟨111⟩	7·223	Y	14^3
Mo	Crowdion	7·187	Y	14^3
W	⟨100⟩	9·815	Y	14^3
W	⟨110⟩	9·641	Y	14^3
W	⟨111⟩	8·919	Y	14^3
W	⟨111⟩	8·908	Y	14^3
W	Crowdion	**8·893**	Y	14^3
W	Crowdion	**8·881**	Y	16^3
W	Crowdion	**8·875**	Y	18^3

† Y = yes, N = no.
‡ See the text for an explanation.

When the core is included, total energies rise considerably for all interstitial configurations, as can be seen by comparing the two Ta sections in table 3. The two ⟨111⟩ defects (the ⟨111⟩ crowdion and the ⟨111⟩ split dumb-bell interstitial) now have almost the same energy, and the minimum is shifted to the ⟨110⟩ orientation. Figure 8 plots the formation energy against orientation once the core has been introduced. The new relaxed positions lead to change in shape of the cohesive part. This now dominates, and a stable ⟨110⟩ configuration arises.

Fig. 7
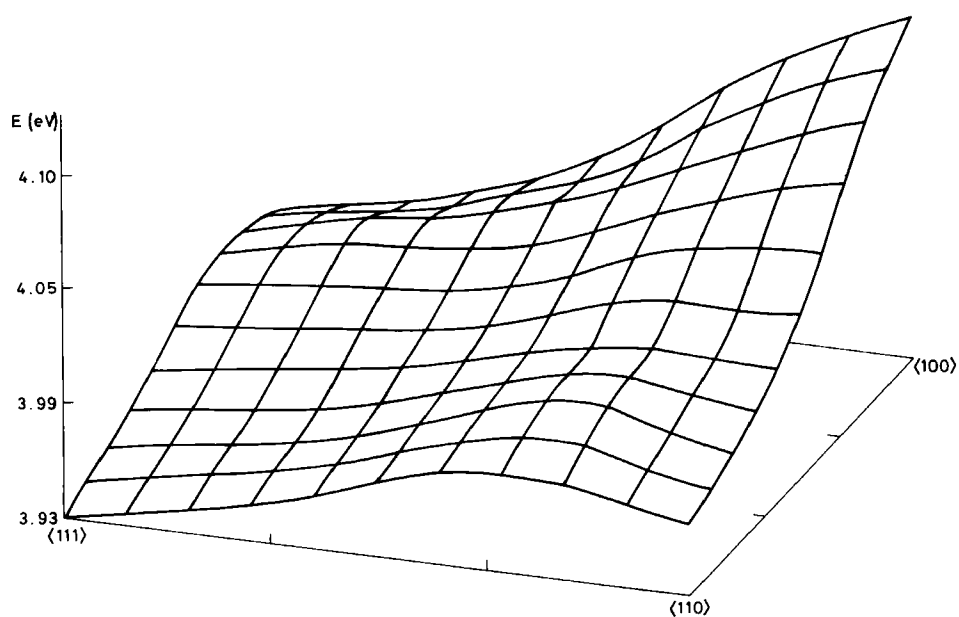
Tantalum without core: interstitial formation energy against orientation.

Fig. 8
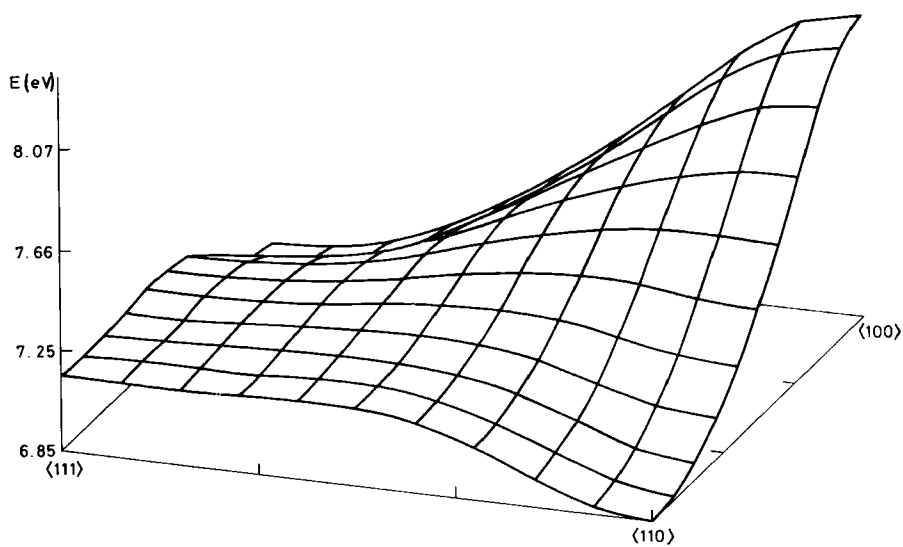
Tantalum with core: interstitial formation energy against orientation.

6.3. *Vanadium and niobium: the effect of the core*

As mentioned in § 5.1, the potentials for V and Nb as originally published lead to an instability in a lattice structure; hence the absence of these metals from the work of Harder and Bacon (1986), and the difficulties experienced earlier when trying to perform relaxations with DEVIL. The inclusion of the core allows calculations to be carried out, and the results obtained with DEVIL are given in table 3. For both metals, a plot of interstitial formation energy against dumb-bell orientation looks similar to that for tantalum given in fig. 8, although in niobium the ⟨111⟩ energy is approximately equal to the ⟨100⟩ energy. Both have deep minima at ⟨110⟩, and relax quickly to this configuration from anywhere nearby.

One relaxation was carried out for V with the atoms starting very near to the positions used to generate the crowdion, but with a slight asymmetry. After about 120 lattice energy evaluations, compared with the 30 or 40 usually required for convergence, the lattice had relaxed to the ⟨110⟩ split dumb-bell configuration. A crowdion calculation was also made on a 16^3 block, for comparison with the usual 14^3 region. The crowdion was selected as it is the most extended defect, and so is most likely to be constrained by a small block. As table 3 shows, the energy was reduced by only 8 meV, indicating that the 14^3 calculation gives acceptable results. In fact, we have found that, for an interstitial in a general b.c.c. metal, a good rule of thumb is that the energy difference between 16^3 and 18^3 is approximately half that between 14^3 and 16^3, and keeps halving as the block size is increased in steps of two lattice planes. For V, this suggests that the formation energy of the crowdion in an infinite block is about 5·585 eV.

### 6.4. *Tungsten: a stable crowdion and one-dimensional migration*

All of the metals so far described have a stable dumb-bell in the ⟨110⟩ direction, or near to it, once the core has been included. Tungsten, however, is different. Although a ⟨111⟩ dumb-bell is a minimum of the energy, and the lattice will relax into this configuration if started near to it, the absolute energy minimum is that of the crowdion.

The fact that the crowdion configuration is close to that of the ⟨111⟩ dumb-bell suggests that interstitial migration along the ⟨111⟩ direction should be the preferred route in tungsten. For a dumb-bell to rotate from (111) to (11$\bar{1}$) via (110) (the lowest-energy path), an activation energy of 0·72 eV (table 3 and fig. 9) must be overcome. For the interstitial to move from the crowdion position to the split dumb-bell pointing in the same direction, requires only 0·027 eV (fig. 10).

Block size has an effect on the stability of certain configurations in tungsten. A 14^3 lattice with periodic boundary conditions allows the ⟨111⟩ split dumb-bell to be stable, as does a 16^3 block with fixed boundaries; but a relaxation starting very near to the ⟨111⟩ dumb-bell in a 14^3 block with fixed boundaries will yield the crowdion. The shallow energy minimum at ⟨111⟩ in fig. 10 does not show up because of the coarse grid employed for the calculations.

Some problems were encountered with the modelling of tungsten, arising from the fact that the cohesive part of the potential has a relatively long range. Table 4 gives the ranges of the two parts of the potential in terms of the cube edge distance, and it can be seen that the range of the cohesive part in W comes close to the third-neighbour distance of $a\sqrt{2} \simeq 1·414a$. A small distortion of the lattice can therefore bring the third neighbours into range, causing problems for a program like DEVIL which works on the neighbour-list principle. It was necessary to write a module to go through the relaxed configuration of the lattice, check for any extra interactions which had not

Fig. 9
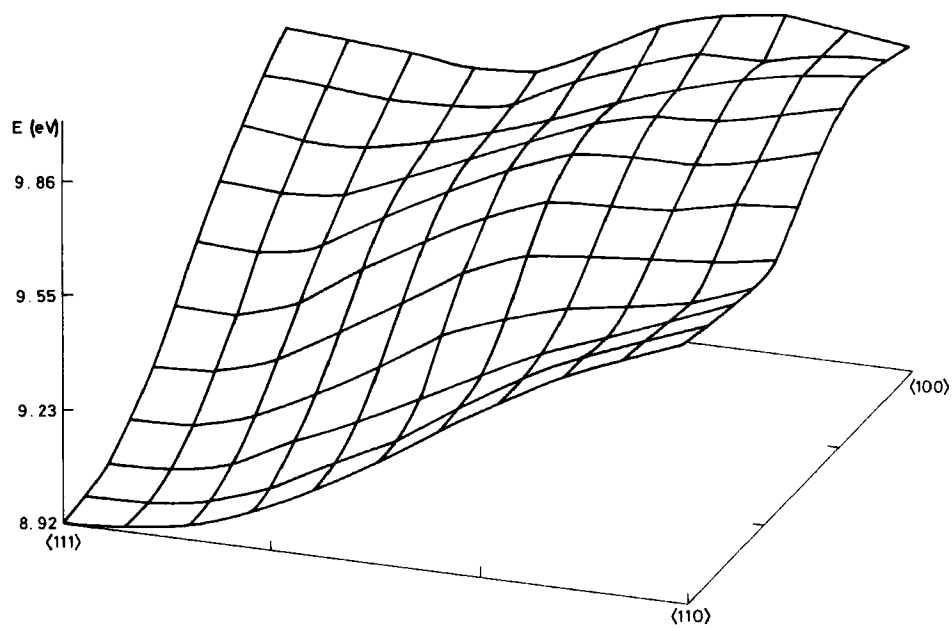
Tungsten: interstitial formation energy against dumb-bell orientation.

Fig. 10
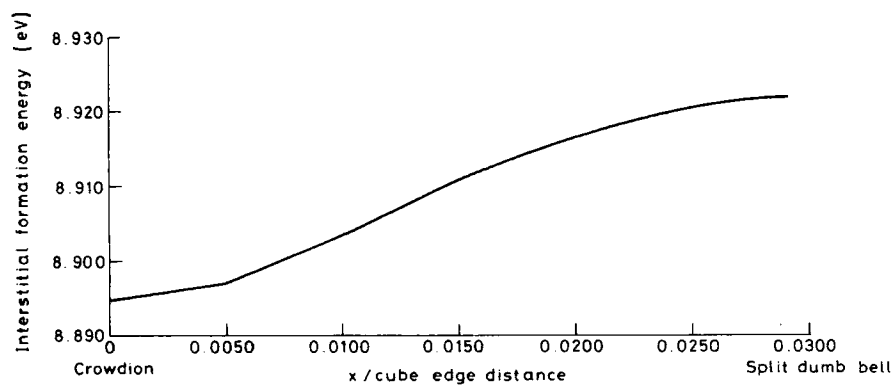
Energy of migration in the $\langle 111 \rangle$ direction for a tungsten interstitial. x is the difference of each coordinate of the interstitial position from that of the crowdion (0·25 0·25 0·25).

Table 4. Ranges of the cohesive and repulsive parts of the potential.

Metal	a (Å)	r_{coh}/a	a_{rep}/a
V	3·0399	1·214766	1·250
Nb	3·3088	1·186183	1·272
Ta	3·3058	1·233281	1·270
Mo	3·1472	1·307456	1·033
W	3·1652	1·390188	1·027

previously been considered, and write appropriate warning messages. This indicated that many third-neighbour interactions were present, and the search distance for constructing the neighbour-list had to be increased to encompass all such interactions.

6.5. *Molecular dynamics*

Quenched molecular dynamics (MD) simulations, with periodic, constant-pressure boundary conditions, have been made for interstitials in all of the metals studied in this paper. The molecular dynamics program uses the Parrinello–Rahman Lagrangian to allow for the variable cell size (Parrinello and Rahman 1980, 1981); the link-cell method of finding neighbours (Fincham and Heyes 1985); and the Gear predictor–corrector scheme to integrate the equations of motion (Gear 1966). The quenching sets to zero the ith component of the velocity of an atom each time the ith component of its acceleration changes sign: i.e. when $v_i a_i < 0$. The molecular dynamic cell is constrained merely to be a parallelepiped. This allows both volume and shear stresses to relax. In the calculation of interstitial formation it is quite important that these degrees of freedom are available. For a typical 16^3 block, they lower the energy by about 0·03 eV, compared with constant-volume zero-shear configurations. Another advantage of MD is the greater likelihood of locating a global minimum. The lowest energy configurations found by MD are given in table 5, and are compared with the values obtained by static relaxation extracted from table 3. In all cases the energies predicted by MD are slightly lower, but the equilibrium configurations are the same. This gives confidence that the static relaxations are not converging to a local minimum and missing a global minimum.

A typical DEVIL relaxation of a 16^3 block to give the energy correct to 10^{-4} eV, needs about 40 calls of the function which evaluates the lattice energy, and 16 seconds of

Table 5. Comparison of interstitial formation energies and configurations obtained by molecular dynamics, and energies from DEVIL. All of the MD calculations have a 16^3 block with dynamic boundary conditions, carried out at constant pressure, with the MD block constrained only to remain a parallelepiped. Cores are included.

Metal	Configuration	Formation energy	
		MD	DEVIL
V	⟨110⟩	4·140	4·155
Nb	⟨110⟩	4·447	4·472
Ta	⟨110⟩	6·788	6·828
Mo	Bent	6·957	6·974
W	Crowdion	8·871	8·881

CPU time on a Cray X-MP. A similar calculation using quenched MD requires about 100 time-steps and 90 seconds of CPU time. The expansion of the block delays convergence, because the absolute positions of the atoms are dependent upon the block size.

6.6. *Elastic deformations and interstitial energies*

The introduction of an interstitial induces stresses in a lattice. In calculating the formation energy of a relaxed interstitial it is important to allow this stress to relax as far as possible. With the DEVIL program the volume of the block was fixed at the perfect-lattice value. The calculations using the MD program were initially for a block free to expand and shear, but when a constant-volume constraint was introduced the results were identical to those produced by DEVIL. This is expected since periodic boundary conditions are used in both cases, and the discrepancy between DEVIL and MD results can thus be attributed entirely to elastic strain energy.

From simple continuum elasticity theory it is possible to estimate the effects of relaxing the shear and volume strains. We assume that the equilibrium elastic constants are still valid for the block containing the impurity, and that the strain is homogeneous throughout the block. We can then calculate the elastic energy required to distort the parallelepiped found by MD for a block containing an interstitial, into its initial cuboidal shape. This is, of course, the difference between the DEVIL and MD energies. The method is described in more detail in the Appendix.

The elastic energy calculated this way for Ta is 0·040 eV, which is identical to the difference between the simulation energies in table 5. The fact that the elastic energy is slightly too small corresponds to the stiffening of the elastic constants owing to the interstitial. By far the most important contribution (about 90% of the correction) comes from the bulk modulus term.

§7. CONCLUSIONS

Fitting of repulsive cores to the pair-potential part of the FS potentials has been shown to be necessary if meaningful atomistic simulations are to be carried out. The cores presented for the five b.c.c. metals V, Nb, Ta, Mo and W seem to lead to sensible properties of the metals. We note that FS potentials were also derived for Fe and Cr, but their stability has not yet been investigated. The pressure–volume curves appear to be realistic, and simulation of V and Nb has become possible. The additions to the potential are based on electron gas potentials of the Wedepohl type.

The stability of the b.c.c. crystal structure has been examined (Ackland and Finnis 1986) against a number of other possible structures for these potentials. Since the only alteration to the potentials is an extra repulsive term, and the energy of b.c.c. remains unchanged at zero pressure, these calculations are still valid. The successful application of molecular dynamics techniques provides further evidence of overall b.c.c. stability.

Formation energies have been obtained for various interstitial configurations, and compared with the theoretical work of other authors. Inclusion of the core has a significant effect in some cases, altering which of the possible symmetry positions has the lowest energy. The results of selected static relaxations have been compared with those from a molecular dynamics program.

The results obtained from the many-body potential suggest that one-dimensional migration of interstitials will take place in tungsten, along the $\langle 111 \rangle$ direction. This conclusion is based on the rather sparse migration calculations so far carried out, with only a small region round the $\langle 111 \rangle$ migration path so far investigated. Further calculations are under way, for tungsten and for other metals.

We recommend that any future modelling work on V, Nb, Ta, Mo or W should include the extra repulsive core presented here.

APPENDIX

Elasticity theory

The difference between the energies calculated for an interstitial in a fixed-volume block, and those for an interstitial in a fixed-pressure block, can be estimated by elasticity theory.

We consider the cubic shape of the DEVIL block to have been obtained by homogeneous deformation of the fully relaxed (MD) block. This distortion can be described by the six independent strain parameters e_{xx}, e_{yy}, e_{zz}, e_{xy}, e_{xz}, e_{yz}.

The free energy of this distortion can be expanded in powers of e_{ij}, though the number of terms in each order is restricted by symmetry considerations. At equilibrium the first-order terms are zero, so in this calculation we consider only second-order terms. Assuming that the distortion of the lattice is too small to break the four-fold symmetry, there are three independent second-order elastic constants. Here we consider C', C_{44} and B, in terms of which the free energy can be written

$$
\begin{aligned}
U_{el} = {} & \tfrac{1}{2}B(e_{xx}+e_{yy}+e_{zz})^2 \\
& + \tfrac{1}{2}C'[\tfrac{1}{3}(2e_{zz}-e_{xx}-e_{yy})^2 + (e_{xx}-e_{yy})^2] \\
& + \tfrac{1}{2}C_{44}(e_{xy}^2+e_{xz}^2+e_{yz}^2).
\end{aligned}
\tag{A 1}
$$

By symmetry, for all $\langle 110 \rangle$ dumb-bell interstitials, the relaxed MD block has $e_{xx}=e_{yy}$ and $e_{yz}=e_{xz}$. We can therefore write

$$
U_{el} = \tfrac{1}{2}B(2e_{xx}+e_{zz})^2 + \tfrac{1}{3}C'(e_{zz}-e_{xx})^2 + \tfrac{1}{2}C_{44}(e_{xy}^2+2e_{xz}^2).
\tag{A 2}
$$

The first term in eqn. (A 2) is the only one associated with a volume change. It is by far the largest, typically 90% of U_{el}. The second term can be viewed as a linear stretch, while the third term represents the distortion of the box away from a rectangular shape.

REFERENCES
ACKLAND, G. J., and FINNIS, M. W., 1986, *Phil. Mag.* A, **54**, 301.
BOLEF, D. I., 1961, *J. appl. Phys.*, **32**, 100.
CARTER, W. J., MARSH, J. N., FRITZ, J. N., and McQUEEN, R. G., 1971, *U.S. Natl Bur. Standards Spec. Publ.*, **326**, p. 147.
FINCHAM, D., and HEYES, D. M., 1985, *Advances in Chemical Physics*, Vol. LXIII (New York: John Wiley), pp. 493–575.
FINNIS, M. W., and SINCLAIR, J. E., 1984, *Phil. Mag.* A, **50**, 45.
GEAR, C. W., 1966, ANL Report 7126, Argonne National Laboratory.

GORDON, R. G., and KIM, Y. S., 1972, *J. chem. Phys.*, **56**, 3122.

GRAHAM, L. J., NADLER, H., and CHANG, R., 1968, *J. appl. Phys.*, **39**, 3025.

HARDER, J. M., and BACON, D. J., 1986, *Phil. Mag.* A, **54**, 651.

HARDING, J. H., and HARKER, A. H., 1982, AERE Report R10425 (London: HMSO).

HARRIS, J., and JONES, R. O., 1979, *J. chem. Phys.*, **70**, 830.

HERMAN, F., and SKILLMAN, S., 1963, *Atomic Structure Calculations* (Englewood Cliffs, N.J.: Prentice-Hall).

HUBER, K. P., and HERZBERG, G. L., 1979, *Molecular Spectra and Molecular Structure, Constants of Diatomic Molecules* (New York: Van Nostrand Reinhold).

JENSEN, H., 1932, *Z. Physik*, **77**, 722; 1936, *Ibid.*, **101**, 164.

KATAHARA, K. W., MANGHANANI, M. H., and FISHER, E. S., 1976, *J. appl. Phys.*, **47**, 434.

LEISURE, R. G., HSU, D. K., and SEIBER, B. A., 1973, *J. appl. Phys.*, **39**, 3394.

LENZ, W., 1932, *Z. Physik*, **77**, 713.

MAO, H. K., BELL, P. M., SHANER, J. W., and STEINBERG, D. J., 1978, *J. appl. Phys.*, **49**, 3276.

MATTHAI, C. C., and BACON, D. J., 1985, *Phil. Mag.* A, **52**, 1.

MERX, H., and MOUSSIN, C., 1980, *Proceedings of the Seventh International AIRAPT Conference*, Pt. 1, Le Creusot, France, 1979 (Oxford: Pergamon), pp. 204–220.

MAYSENHÖLDER, W., 1986, *Phil. Mag.* A, **53**, 783.

PARRINELLO, M., and RAHMAN, A., 1980, *Phys. Rev. Lett.*, **45**, 1196; 1981, *J. appl. Phys.*, **52**, 7182.

THETFORD, R., 1985, Harwell Report AERE M3507 (London: HMSO).

WEDEPOHL, P. T., 1967, *Proc. phys. Soc.*, **92**, 79.

XU, J., MAO, H. K., and BELL, P. M., 1984, *High Temp. high Press.*, **16**, 495.

ZEPER, W. B., 1986, Dissertation, Technische Hogeschool Delft.